Available online at www.sciencedirect.com
ScienceDirect
Journal of Sound and Vibration 304 (2007) 660–676
JOURNAL OF SOUND AND VIBRATION
www.elsevier.com/locate/jsvi

Estimation of cable tension force using the frequency-based system identification method

Byeong Hwa Kim[a], Taehyo Park[b,*]

[a]*Steel Structure Research Lab., Research Institute of Industrial Science & Technology, 79-5 Yeongcheon, Dongtan, Hwaseong, Gyeonggi, 445-813, Republic of Korea*
[b]*Department of Civil Engineering, Hanyang University, 17 Haengdang-dong, Seoul 133-791, Republic of Korea*

Received 1 November 2006; accepted 6 March 2007
Available online 26 April 2007

Abstract

This work proposes a new technique to estimate cable tension force from measured natural frequencies. The proposed method is able to simultaneously identify tension force, flexural rigidity, and axial rigidity of a cable system. Firstly, a finite element model that can consider both sag-extensibility and flexural rigidity is constructed for a target cable system. Next, a frequency-based sensitivity-updating algorithm is applied to identify the model. The proposed approach is applicable to a wide range of a cable system that is beyond the applicable limits of the existing methods. From the experimental works, it is seen that the tension force is determined with an accuracy of 3% by the proposed approach. Furthermore, it is observed that the flexural rigidity of cable with high bending stiffness is proportional to the applied tension force.

1. Introduction

Modern advances in material, analysis, and construction technology have resulted in increasing number of a long-span cable bridge. Since cables are a crucial element for overall structural safety of the structure, the accurate measurement of cable tension force has practical importance to not only a construction stage but also a maintenance stage. Currently available techniques to estimate the cable tension include the static methods directly measuring the tension by a load cell or a hydraulic jack, and the vibration methods indirectly estimating the tension from measured natural frequencies. In practice, the vibration methods have received increasing attention because of its simplicity and speediness.

Depending on whether the sag-extensibility and bending stiffness are taken into account or not, the existing vibration methods may be classified as the following four categories. The first category utilizes the flat taut string theory that neglects both sag-extensibility and bending stiffness:

$$T = 4mL^2\left(\frac{f_n}{n}\right)^2, \tag{1}$$

*Corresponding author. Tel.: +82 2 2220 0321; fax: +82 2 2293 9977.
E-mail address: cepark@hanyang.ac.kr (T. Park).

0022-460X/$ - see front matter © 2007 Elsevier Ltd. All rights reserved.
doi:10.1016/j.jsv.2007.03.012

where f_n denotes the nth natural frequency in Hz. The terms T, m, and L denote tension force, mass density, and length of cable, respectively. Given the measured frequency and the mode number, the computation of tension force is straightforward. However, the application of this formula is strictly limited to a flat long slender cable. The second category makes use of the modern cable theory [1–3] that takes account of the sag-extensibility without bending stiffness. This approach requires additional information of the unstrained length of cable and involves solving a nonlinear characteristic equation by trial-and-error [4]. However, such additional information is often not available in practice. The third category utilizes the following frequency formula of an axially loaded beam that considers the bending stiffness but neglects the sag-extensibility:

$$\left(\frac{f_n}{n}\right)^2 = \left(\frac{1}{4mL^2}\right)T + \left(\frac{n^2\pi^2}{4mL^4}\right)EI, \tag{2}$$

where EI denotes the flexural rigidity of a cable. Given the measured frequency and the mode number, the linear regression procedures are applied to identify unknown tension force and flexural rigidity simultaneously. This approach is often used by the field engineers because of its simplicity and speediness. The last category takes account of both sag-extensibility and bending stiffness using a practical formula [5–7]. For the proper use of the proposed formula, a priori knowledge of the axial rigidity and flexural rigidity of the target cable system is required. However, in practice, the flexural rigidity of cable is often neither available nor valid since the shear and bending mechanisms of a cross section of a cable could be different from those of a beam.

The aforementioned vibration methods have at least the following three shortcomings related to their applicable limits. First, the existing vibration methods are based on a closed form relationship between cable tension force and the natural frequencies for a simple mathematical model. Hence, it is not surprising to get accurate estimation of tension force if the target cable system is well represented by the model. However, the estimation result may be significantly distorted if the model could not accurately describe the behavior of the target cable system. For instance, the application of the taut string theory in Eq. (1) to a cable with high sag and high bending stiffness does not guarantee the good results of the estimated cable tension force. Neither does the application of the modern cable theory to a short thick cable such as the tie-rod of an arch bridge. In general, the influence of cable extensibility is negligible for short thick cables but could lead to important errors for long sagged cables [8]. Here, the short thick cables belong to a class of cables that is not slender or not sufficiently tensioned. For such short thick cables, the higher natural frequencies are greater than predicted by the taut string theory, as shown in Tsing Ma Bridge [9]. Second, the existing vibration methods may not be applicable to the cable system whose analytical solution is not known. For instance, the existing vibration methods may not be applicable to the inclined double short hanger of a suspended bridge that consists of two independent cables tied by a clamp and a spacer. Although an application of Eq. (2) to cables with a transverse connector is found [10], such an application is strictly limited to relatively long cables of which the tied-effects are negligible. Third, some vibration methods require not only the measured frequencies but also additional information such as cable effective length and material parameters. However, such additional information that affects accuracy of the resulting tension force is often not available in practice. Therefore, there remains a need to resolve these deficiencies of the existing vibration methods.

The objective of this paper is to introduce a new technique that can estimate cable tension force from measured natural frequencies. The proposed approach resolves the aforementioned deficiencies of the earlier approaches by using a finite element analysis technique and applying a system identification technique [11]. Here, the finite element analysis is adopted in order to extend the applicable limits on geometric complexity of a target cable system, and the state-of-the-art system identification technique is applied in order to overcome the required knowledge of material properties and static shapes of cables. To achieve the objective, the following three tasks are performed. First, the approach to estimate cable tension force from the measured natural frequencies is outlined. Second, a set of numerical comparative study is conducted to examine the accuracy of the proposed approach. Third, the feasibility and practicability of the proposed approach are examined by the laboratory experiments and a field application.

2. Theory

Suppose that the mass density and boundary condition of a cable are known. Given the measured natural frequencies, this paper deals with the problem how to identify the horizontal component of tension force, flexural rigidity, and axial rigidity of a cable system. Note that the horizontal force, instead of tension force, is selected for an identification variable. The reason is attributed to the fact that the horizontal force is a constant while the derivatives of tension force cannot be neglected for a large-sagged cable. In addition, the reason for selecting the flexural rigidity and axial rigidity of a cable is that such material properties are often unavailable or invalid in some practical cases. For instance, the shear and bending mechanism of a cable element may not be the same with that of a continuum structure because the cross section of most structural cables consists of individual strands or wires. Also, Ni et al. [9] shows that the flexural rigidity significantly affects the higher frequencies of a large-diameter sagged cable.

Consider a $p \times 1$ identification variable vector $\mathbf{U}$ that consists of the horizontal force H, the flexural rigidity EI, and the axial rigidity EA:

$$\mathbf{U} = \begin{bmatrix} H & EI & EA \end{bmatrix}^{\mathrm{T}}. \tag{3}$$

Then, the nth eigenvalue β_n can be described by a function of the identification variable vector. The Taylor expansion of the nth eigenvalue with respect to the identification variable vector is as follows:

$$\beta_n(\mathbf{U} + \mathrm{d}\mathbf{U}) = \beta_n(\mathbf{U}) + \nabla\beta_n(\mathbf{U}) \cdot \mathrm{d}\mathbf{U} + O^2(\mathrm{d}\mathbf{U}). \tag{4}$$

By neglecting the higher order term, the variation of eigenvalue $\delta\beta_n$ can be defined by

$$\delta\beta_n \equiv \beta_n(\mathbf{U} + \mathrm{d}\mathbf{U}) - \beta_n(\mathbf{U}). \tag{5}$$

Then the variation of eigenvalue can be described by

$$\delta\beta_n = \sum_{i=1}^{p} \frac{\partial\beta_n}{\partial U_i} \mathrm{d}U_i, \tag{6}$$

where U_i denotes the ith item of $\mathbf{U}$. For example, U_1 denotes the horizontal force H. For numerical efficiency, Eq. (6) can further be normalized by

$$\frac{\delta\beta_n}{\beta_n} = \sum_{i=1}^{p} \frac{\partial\beta_n}{\partial\beta_i} \frac{U_i}{\beta_n} \frac{\mathrm{d}U_i}{U_i}. \tag{7}$$

If the number of measured natural frequencies is q, Eq. (7) can be conveniently written by

$$\mathbf{Z} = \mathbf{F}\boldsymbol{\alpha}, \tag{8}$$

where the $q \times 1$ vector $\mathbf{Z}$ is the variation of eigenvalue denoted by

$$\mathbf{Z} = \begin{bmatrix} \dfrac{\delta\beta_1}{\beta_1} & \cdots & \dfrac{\delta\beta_q}{\beta_q} \end{bmatrix}^{\mathrm{T}}. \tag{9}$$

The $p \times 1$ vector $\boldsymbol{\alpha}$ is the fractional changes in the identification variables denoted by

$$\boldsymbol{\alpha} = \begin{bmatrix} \dfrac{\mathrm{d}U_1}{U_1} & \cdots & \dfrac{\mathrm{d}U_p}{U_p} \end{bmatrix}^{\mathrm{T}}. \tag{10}$$

The $q \times p$ vector $\mathbf{F}$ is the sensitivity matrix denoted by

$$\mathbf{F} = \begin{bmatrix} \dfrac{\partial \beta_1 U_1}{\partial U_1 \beta_1} & \cdots & \dfrac{\partial \beta_1 U_p}{\partial U_p \beta_1} \\ \vdots & \ddots & \vdots \\ \dfrac{\partial \beta_q U_1}{\partial U_1 \beta_q} & \cdots & \dfrac{\partial \beta_q U_p}{\partial U_p \beta_q} \end{bmatrix}. \tag{11}$$

The iterative solution procedure of Eq. (8) consists of the following seven steps. First, assume an arbitrary identification variable vector at the kth iteration step:

$$\mathbf{U}^k = \begin{bmatrix} H^k & EI^k & EA^k \end{bmatrix}^{\mathrm{T}}, \tag{12}$$

where the superscript denotes the iteration number. Second, compute a static profile and the distribution of tension force caused by the self-weight of the cable. For a cable system with high sag and high bending stiffness, a nonlinear finite element analysis is required [9]. If the sag-to-span ratio of the cable is less than 1/8, the desired static profile could be readily approximated by the parabola with sufficient accuracy [1]. Third, perform the eigenvalue analysis for the resulting deformed and stressed cable. Fourth, compute the sensitivity matrix $\mathbf{F}$ in Eq. (11) by approximation. Here, the p times eigenvalue analyses are required for a unit change of U_i. Fifth, compute the fractional change of eigenvalue $\mathbf{Z}$ by using the following equation:

$$\mathbf{Z} = \begin{bmatrix} \dfrac{\beta_1^t - \beta_1^k}{\beta_1^k} & \cdots & \dfrac{\beta_n^t - \beta_n^k}{\beta_n^k} & \cdots & \dfrac{\beta_q^t - \beta_q^k}{\beta_q^k} \end{bmatrix}^{\mathrm{T}}, \tag{13}$$

where β_n^t denotes the nth measured target eigenvalue. β_n^k denotes the nth eigenvalue at the kth iteration step resulted from the third step above. Sixth, compute the fractional changes in the identification variables by using the following equation:

$$\boldsymbol{\alpha} = \mathbf{F}^{-1}\mathbf{Z}, \tag{14}$$

where $\mathbf{F}^{-1}$ denotes a pseudo inverse matrix of $\mathbf{F}$ that can be approximated by

$$\mathbf{F}^{-1} = \lim_{\boldsymbol{\varepsilon} \to \mathbf{0}} \left[\mathbf{F}^{\mathrm{T}}\mathbf{F} + \boldsymbol{\varepsilon}\right]^{-1}\mathbf{F}^{\mathrm{T}}. \tag{15}$$

Eq. (8) is supposed to be over-determined ($p < q$). Since the pseudo-inverse solution in Eq. (14) is based on a least-square technique, the number of measured modes should be larger than that of the identification variables in order to avoid the uniqueness problem [12]. Seventh, update the identification variables of the $(k+1)$th iteration step by

$$U_i^{k+1} = (1 + \alpha_i^k) U_i^k, \tag{16}$$

where U_i^k denotes the ith identification variable of $\mathbf{U}^k$ at the kth iteration step, and α_i^k denotes the ith element of $\boldsymbol{\alpha}$ at the kth iteration step. These seven steps are repeated until the fractional changes of the identification variable α_i converge to zeros.

3. Numerical study

Consider an inclined cable with two hinged ends shown in Fig. 1. The mass density per unit length of the cable m is 400 kg/m. The horizontal span length l is 100 m. The angle of the cord θ is 30°. The sag-extensibility

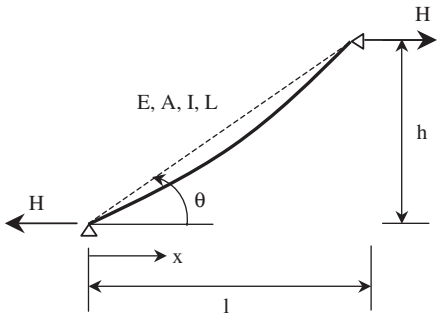

Fig. 1. Inclined cable.

Table 1
Structural properties of four inclined cables

Cable no.	λ^2	ξ	H (MN)	E (GPa)	A ($\times 10^{-3}$ m^2)	I ($\times 10^{-6}$ m^4)
1	0.68	605.5	2.9036	15.988	7.8507	4.9535
2	44.00	302.7	0.7259	17.186	7.6110	4.6097
3	1.22	50.5	26.1325	20826.	7.8633	4.9204
4	44.00	50.5	0.7259	0.048	273.45	5950.6

parameter λ^2 and bending stiffness parameter of a cable ξ is defined by [1]

$$\lambda^2 = \left(\frac{mgl\sec\theta}{H}\right)^2 \frac{EA}{H}\frac{l}{L_e},$$

where

$$L_e = l\sec^3\theta\left[1+\frac{1}{8}\left(\frac{mgl}{H}\right)^2\right], \tag{17}$$

$$\xi = l\sqrt{\frac{H}{EI}}. \tag{18}$$

The proposed method is applied to the four cables in Table 1. For comparison, the cable properties of the chosen cables are similar to those of the horizontal cables used in Refs. [7,9]: Cable 1 represents a cable with moderate sag and low bending stiffness; Cable 2 represents a cable with very high sag and average bending stiffness; Cable 3 represents a cable with moderate sag and high bending stiffness; Cable 4 represents a cable with high sag and high bending stiffness. It is assumed that the first 20 lower eigenvalues of the lateral in-plane motion are measured by vibration tests. From such measured frequencies, the variables supposed to be identified are the horizontal component of cable tension force H, the flexural rigidity EI, and the axial rigidity EA. Here, the selected initial values of the horizontal force, the flexural rigidity, and the axial rigidity are 50%, 110%, and 90% of the exact values, respectively. For convenience, the deflected static profiles of the cables are assumed to be parabolic. For eigenvalue analyses, a linear finite element of an axially loaded beam is developed in the MATLAB® code. For each iteration step, the identified variables of Cable 1 are shown in Fig. 2. In Fig. 2a, the terms α_1, α_2, and α_3 denote the fractional changes in the horizontal components of cable tension force, the flexural rigidity, and the axial rigidity, respectively. It is seen that the horizontal forces and the axial rigidity rapidly converges while the flexural rigidity slowly converges. The reason of this slow convergence is due to the fact that the sensitivity of the bending stiffness to the frequencies is very small because Cable 1 has low bending stiffness. However, all the identification variables of Cable 4 have rapidly converged to zero within 10 iterations because Cable 4 has high sag and high bending stiffness. For Cable 1,

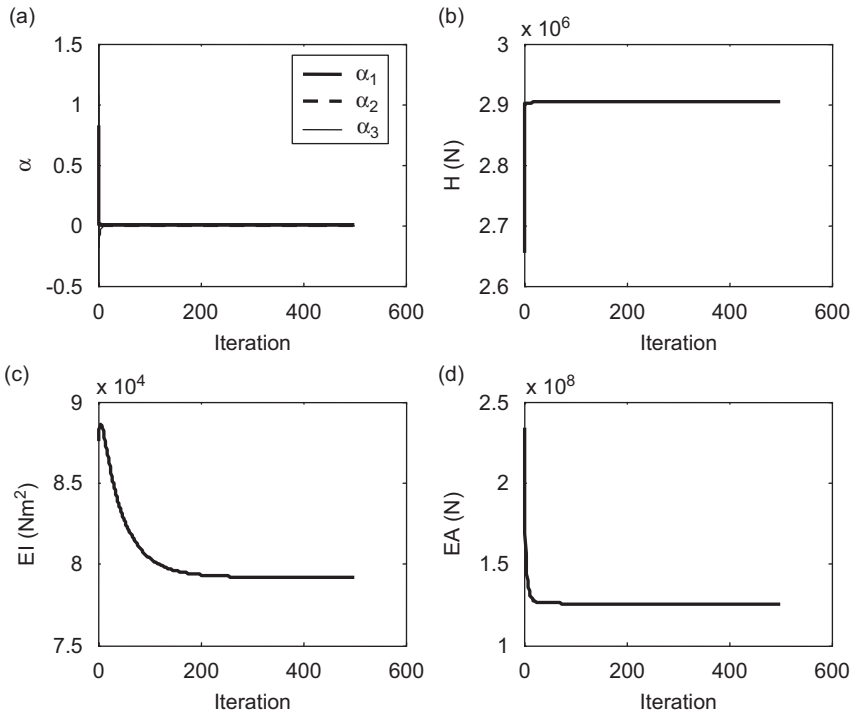

Fig. 2. Convergence of identification variables of Cable 1: (a) fractional changes; (b) horizontal force component; (c) bending stiffness; and (d) axial stiffness.

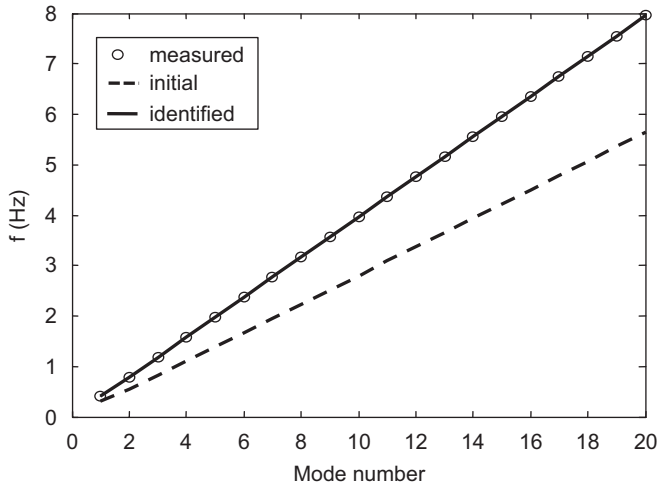

Fig. 3. Comparison of the identified natural frequencies of Cable 1.

Fig. 3 shows the good agreements between the measured frequencies and the frequencies computed by the finally converged variables. Also, the sag-extensibility parameters and bending stiffness parameters computed by the identified variables are $\lambda^2 = 0.68$ and $\xi = 605.5$, respectively. These results agree well with the exact values in Table 1.

The cable tension forces for Cable 1 estimated by the existing methods are shown in Fig. 4. For the taut string theory (Eq. (1)) and the modern cable theory [4], the estimated tension force using the first mode yields the relatively larger deviation from the exact tension force than the higher modes. The average errors of the

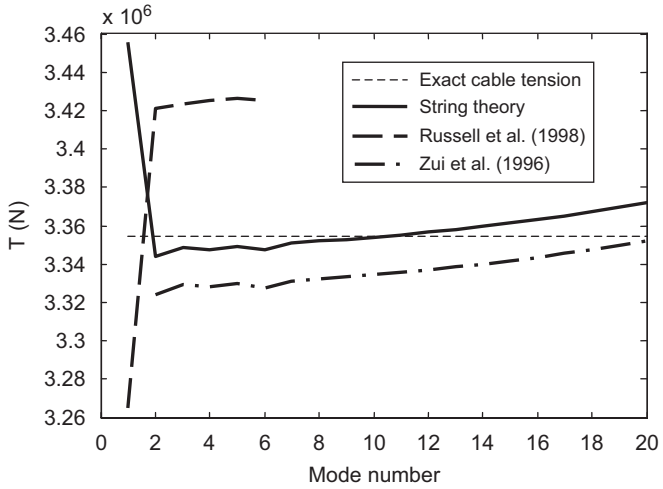

Fig. 4. Comparison of cable tension forces estimated by the existing methods.

Table 2
Estimation results of cable tension force of four cables ($\times 10^6$ N)

	Cable no.			
	1	2	3	4
Exact tension	3.35	0.84	30.18	0.84
Proposed approach	3.35 (0.0)	0.84 (0.0)	30.18 (0.0)	0.84 (0.0)
String theory (Eq. (1))	3.36 (−0.2)	0.92 (−9.2)	41.11 (−36.3)	1.21 (−43.2)
Russell et al. [4]	3.40 (−1.3)	0.70 (17.0)	31.46 (−4.3)	0.73 (13.4)
Linear regression (Eq. (2))	3.35 (0.2)	0.83 (1.5)	30.13 (0.14)	0.83 (1.5)
Zui et al. [5]	3.17 (5.5)	0.79 (6.2)	28.34 (6.08)	0.79 (6.1)

Note: ( ) is % error.

estimation results of the taut string theory and the modern cable theory are only −0.2% and −1.3%, respectively. These good results are natural because Cable 1 has moderate sag and low bending stiffness. As shown in Table 2, however, their estimation results significantly degenerate in Cable 4 because of high sag and bending stiffness. For the practical formula by Zui et al. [5], the error level of 6% seems to be consistent for all cables. For Cable 1, the estimation process of the linear regression approach in Eq. (2) is shown in Fig. 5. The first mode largely deviates from the linear regression line obtained by 20 modes. This results in 77.01% error of the flexural rigidity computed by the slope of the regression line. However, the error of cable tension force estimation is negligibly small. Excluding the lower five modes, the error of the flexural rigidity estimation significantly decreases by 4.83% as shown in Table 3. The reason of this improvement is attributed to the fact that the sag-extensibility mostly affects the lower modes. This indicates that the linear regression approach requires the higher modes for a sagged cable.

Based on Table 2, the application of the taut string theory is very limited to cables with low sag-extensibility and low bending stiffness. However, the taut string theory could be used as a maximum bound of cable tension force due to a tendency of over-estimation and its practicability. For the method by the modern cable theory, the error of the tension force estimation tends to increase as sag-extensibility and bending stiffness increase. For the tension estimated by the linear regression approach, the error increases as a sag-to-span ratio increases. Its accuracy is typically good if the first five lower modes are excluded. However, as shown in Table 3, the error of the flexural rigidity estimation tends to increase as the bending stiffness decreases. For the practical formulas proposed by Zui et al. [5], the ranges of errors are around 6%. Furthermore, the resulting

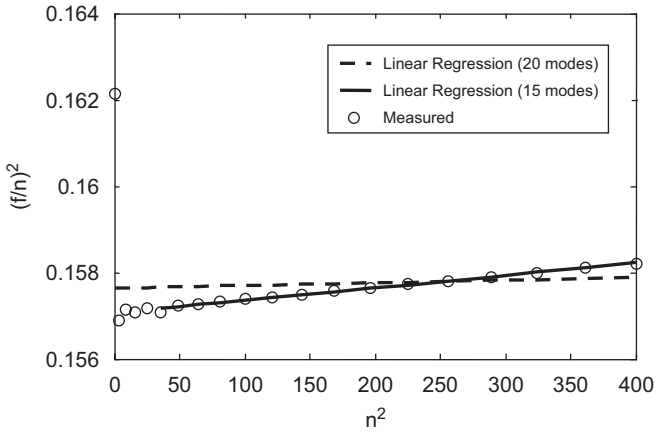

Fig. 5. Comparison of cable tension forces estimated by linear regression method.

Table 3
Estimation results of bending stiffness of four cables ($\times 10^4\,\mathrm{Nm}^2$)

	Cable no.			
	1	2	3	4
Exact flexural rigidity	7.92	7.92	10247	284.64
Proposed approach	7.92 (0.0)	7.92 (0.0)	10247 (0.0)	284.64 (0.0)
Linear regression	8.30 (−4.8)	8.28 (−4.5)	10253 (−0.1)	278.29 (2.2)

Note: ( ) is % error.

tension force tends to be underestimated. However, for all cables, the proposed approach shows the 0.0% errors of cable tension force, the flexural rigidity, and the axial rigidity.

4. Experiments

To verify the proposed approach, an experimental verification task is conducted for a laboratory model that scales a cable-stayed bridge. As shown in Fig. 6, the steel frame of the model consists of a column and a beam that represent a pylon and a slab deck, respectively. To support the applied tension force, all the connections of the frame are welded. By combing weights located below the beam, the tension force is applied to the cable. Duplicating the boundary condition of a cable-stayed bridge, the end of the cable on the pylon side is fixed. To reflect the sag of the cable caused by the applied tension force, a pulley is implemented on the deck side. Without recording the impact force, the cable is excited by an impact hammer of the PCB Piezotronics Model 086C04. The acceleration time history is recorded by an accelerometer installed on the surface of the cable. Here, the implemented accelerometer is the PCB Piezotronics Model 352B10. The data acquisition is conducted with the combination of a Samsung computer GP12, a National Instrument 4472 Board, and self-coded Labview software. The KISWIRE 7×19 galvanized aircraft cable is used in this experiment. The nominal diameter and mass of the cable are $\varnothing 4.76\,\mathrm{mm}$, and $9.67 \times 10^{-2}\,\mathrm{kg/m}$, respectively. The cross sectional area and the moment of inertia of the cable are $1.05 \times 10^{-5}\,\mathrm{m}^2$ and $2.09 \times 10^{-5}\,\mathrm{m}^4$, respectively.

As shown in Table 4, the six vibration tests are repeated with respect to the various levels of applied tension forces. For example, the cable of Test 1 has an applied tension force of 498.35 N (50.85 kgf). Exciting the stressed cable by the impact hammer, the acceleration time histories are collected through the data acquisition system. For Tests 1–3, the acceleration time samples of 5.05×10^5 are recorded for 504.99 s using the sampling

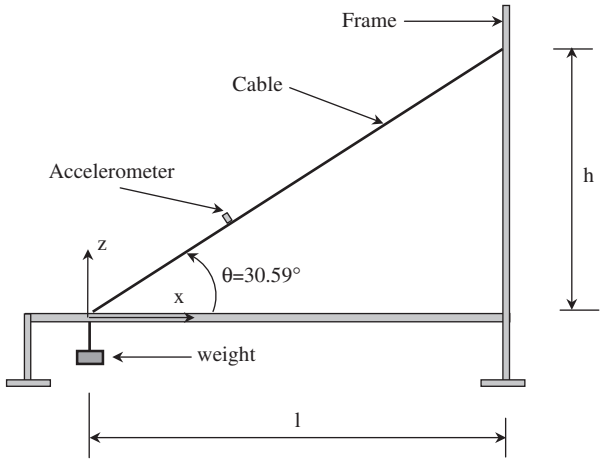

Fig. 6. Laboratory model for a cable-stayed bridge.

Table 4
Applied tension force to the laboratory model

Test no.	Applied weight (N)	Number of modes
1	498.35	19
2	400.25	17
3	302.15	20
4	204.05	14
5	105.95	5
6	17.66	3

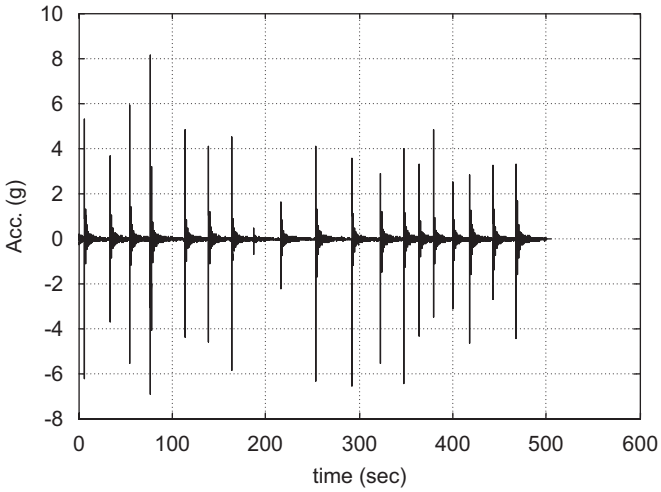

Fig. 7. Time history of accelerometer in Test 1.

frequency of 1000 Hz. For Tests 4–6, the sampling frequency of 500 Hz is used. A typical acceleration time history of Test 1 is shown in Fig. 7. Using the Welch's averaged periodogram method with the Hanning windows, the power spectral densities of the accelerations are shown in Fig. 8. It is seen that only a few of the

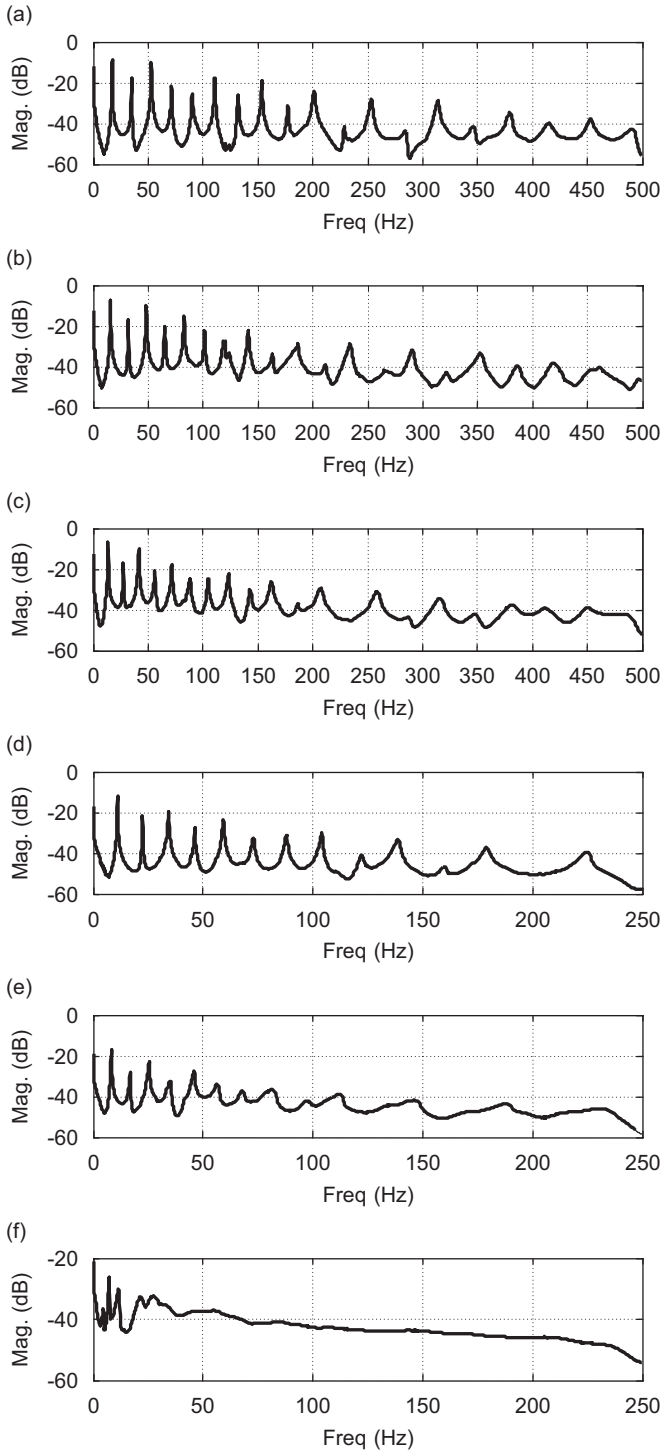

Fig. 8. Spectrum of acceleration: (a) Test 1; (b) Test 2; (c) Test 3; (d) Test 4; (e) Test 5; and (f) Test 6.

lower modes are excited in Test 6. The next step involves extracting the natural frequencies from the measured time histories using the Pick-picking method [13]. The numbers of the extracted natural frequencies are listed in Table 4.

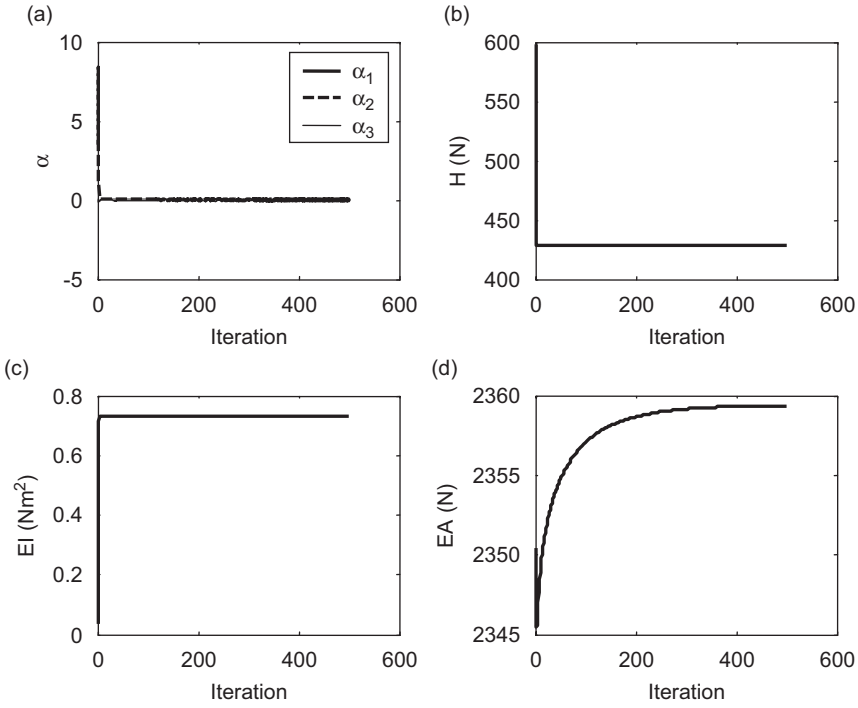

Fig. 9. Convergence of identification variables in Test 1: (a) fractional changes; (b) horizontal force component; (c) bending stiffness; and (d) axial stiffness.

For the accurate estimation of the cable properties, the larger number of measured modes typically guarantees the better reliability, since the proposed identification algorithm is based on L_2 minimization. However, as a rule of thumb, the sag-extensibility and bending stiffness primarily affect the lower and higher modes, respectively.

For the extracted natural frequencies, the proposed approach is applied to estimate applied tension force. Firstly, the initial values of the identification variables are selected. For the initial horizontal forces, the tension forces estimated by the taut string theory are used. For the initial flexural rigidity and the initial axial rigidity, arbitrary values have been chosen. Secondly, the sensitivity-updating algorithm is applied to all the cases of tests. The convergence of the identification variables for Test 1 is shown in Fig. 9. Except the axial rigidity, the other identification variables are rapidly converged within 10 iterations. However, the axial rigidity slowly converges in this experiment. The reason of this slow convergence is due to the fact that the sag-to-span ratio of Test 1 is almost zero due to the relatively large applied tension force. This implies that the effect of sag-extensibility on the natural frequencies is negligibly small for Test 1. However, it is not surprising that the axial rigidity of cable of Test 6 has been rapidly converged within 20 iterations due to a large amount of sag. All the identified variables by the proposed approach are listed in Table 5. It is clearly observed that the bending stiffness increases as the applied tension increases. This indicates that the shear and bending mechanism of cable may not be the same with that of a continuum structure. For all cases, the identified bending stiffness parameters are below 16. This result shows that the bending effect of the cable systems tested could not be neglected. In addition, the identified sag-extensibility parameter has the wide spectrum. This reveals that the sag-extensibility of the cables tested could not be neglected except Test 1.

For the measured natural frequencies, the existing methods are applied to estimate tension forces. As listed in Table 6, the results by the flat taut string theory have the largest error for all cases. Hence, the taut string theory is not acceptable for the cable system tested here. However, the estimated results by the taut string theory could be used as the good maximum bounds of applied tension forces. For the application of the modern cable theory proposed by Russell and Lardner [4], the first six lower frequencies are used from Test 1

Table 5
Identified variables of laboratory model by the proposed method

	Test no.					
	1	2	3	4	5	6
Horizontal force H (N)	429.0	354.7	261.5	174.5	94.2	15.6
Flexural Rigidity EI (Nm^2)	0.73	0.67	0.58	0.51	0.44	0.28
Axial Rigidity EA (kN)	2.36	17.87	0.71	0.95	98.43	28.02
Bending parameter ξ	16.0	15.2	14.0	12.2	9.6	4.9
Sag parameter λ^2	0.09	1.25	0.12	0.56	367.1	23238.0

Table 6
Estimated tension forces of laboratory model (N)

	Test no.					
	1	2	3	4	5	6
Exact tension	498.3	400.2	302.1	204.0	105.9	17.7
Proposed approach	498.4	412.1	303.8	202.7	109.5	18.1
	(0.0)	(3.0)	(0.5)	(−0.7)	(3.3)	(2.4)
String theory (Eq. (1))	718.0	574.9	495.4	287.5	120.9	26.1
	(44.1)	(43.7)	(64.0)	(40.9)	(14.2)	(47.7)
Russell et al. [4]	531.9	440.9	320.4	229.2	120.8	11.90
	(−6.7)	(−10.2)	(−6.1)	(−12.3)	(−14.0)	(37.9)
Linear regression (Eq. (2))	495.8	413.0	304.8	203.3	110.1	30.6
	(−0.5)	(3.2)	(0.9)	(−0.4)	(3.9)	(73.3)
Zui et al. [5]	464.9	375.0	282.8	185.6	96.7	9.9
	(6.7)	(6.3)	(6.4)	(9.0)	(8.8)	(43.8)

Note: ( ) is % error.

to Test 4. For each test, the resulting tension forces are averaged for the six modes and listed in Table 6. For Tests 5 and 6, the first five and three lower frequencies are used and averaged, respectively. It is seen that the results by Russell and Lardner [4] are not very good because of the high bending stiffness of the cable tested. Except Test 6, all the estimated tension forces by the linear regression approach have very good agreements with the measured tension forces. Since the cable of Test 6 has the considerable sag, the occurrence of the large error is predictable. For the approach proposed by Zui et al. [5], the error of the estimated tension forces ranges from 6% to 9% except Test 6. For Test 6, all the existing methods have failed to predict good result. The reason may be traced to the fact that the applied tension force is too low compared to the weight of cable. Note that the total weight of the cable is about 11% of the applied tension force in Test 6. While the existing methods yields considerable errors in the estimation of tension force, the proposed approach shows only about 3% error for all cases.

For the estimated flexural rigidity with respect to the applied tension forces, Fig. 10 shows the comparison between the proposed approach and the linear regression approach. Except Test 6, the estimation results by two approaches are very similar. For Test 6, however, the linear regression approach yields an unrealistic minus value of the flexural rigidity. The reason of this unrealistic result is that only the first three lower frequencies are used in Test 6. Hence, it is obvious that the linear regression approach requires higher modes for accurate estimation of the flexural rigidity. However, the flexural rigidity estimated by the proposed approach gives the reasonable values for all cases.

In Fig. 10, it is seen that the bending stiffness is linearly proportional to an applied tension force. One probable explanation to support to this phenomenon lies in the peculiar mechanism of the shear and bending in the cable structures. Unlike the fundamental engineering beam theory, the horizontal resisting shear stresses

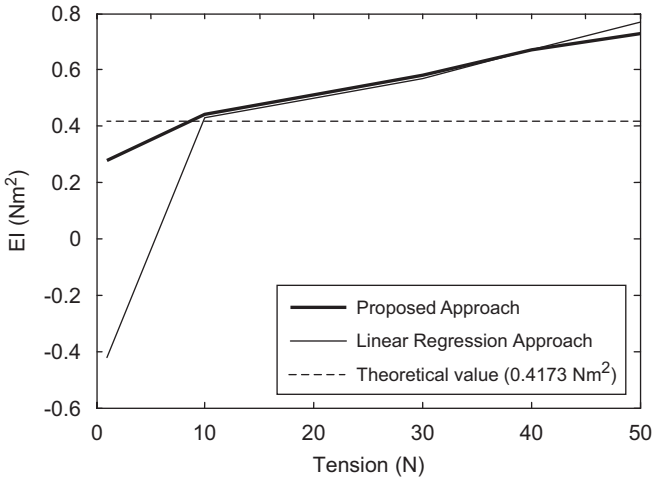

Fig. 10. Estimation results of the flexural rigidity.

between strands or wires might be affected by the transverse compression caused by an applied tension force and the accompanied sag. Consequently, the flexural rigidity of cables increases as tension force increases.

For the estimation of the axial rigidity, there exists a big difference between the proposed approach and the theoretical axial rigidity. This result was not predicted in the previous numerical study. A probable reason is that the sensitivity of the flexural frequencies to the axial rigidity is relatively low for the cable with high bending stiffness. Since the convergence speed of the individual identification variable strictly relies on its sensitivity to frequencies, each identification variable converges differently. As shown in Fig. 9, the horizontal force H and flexural rigidity EI converge in several iterations, but the axial rigidity hardly converges. In this case, the sensitivity of H and EI to cable frequencies is very high, but the sensitivity of EA is very low, because the cable system on Test 1 has high bending stiffness and very low sag. Since the measured frequencies represent the transverse motion, instead of the longitudinal motion, the identification of the axial rigidity from such transverse modes may not be reliable if a cable system has a very low sag-to span ratio. However, in the case of Fig. 2, the identification variables H and EA converge quickly while the flexural rigidity EI converges slowly, because Cable 1 has low bending stiffness and moderate sag. Unlike the axial rigidity, the identification result for the flexural rigidity is very consistent and reliable even if such slow convergence. This is because the flexural rigidity is closely related to the transverse motion. For cables with low sag, the axial rigidity is insensitive to the flexural frequencies. However, the axial rigidity is sensitive to the lower symmetric modes for cables with high sag. To justify this point, the sensitivities of the cable frequencies to the axial rigidity with respect to the various sag-to-span ratios have been investigated. The horizontal cable parameter investigated here are $H = 2.9036\text{MN}$, $E = 15.988\,\text{GPa}$, $A = 7.8507 \times 10^2\,\text{m}^2$, $\xi = 605.5$, $\theta = 0^\circ$, and $L = 100\,\text{m}$, which are similar to Cable 1 in Table 1. As shown in Fig. 11, the sensitivities of the symmetric modes (the 1st, 3rd, and 5th mode, etc.) are sensitive to the axial rigidity when the sag-to-span ratio larger than about 0.02. It is observed that the anti-symmetric modes (the 2th and 4th mode) are completely insensitive to the axial rigidity. Also, the modal crossovers are observed around the sag-to-span ratios of 0.06 and 0.1.

It is also emphasized that the inclusion or the exclusion of the axial rigidity EA in the identification strategy does not affect on the accuracy of tension force identification. Furthermore, the identification error of the axial rigidity EA does not deteriorate the identification accuracy of cable tension force. For cables with high sag, the correct identification of the axial rigidity EA is expected due to the high sensitivity to the lower symmetric modes. For cables with low sag, the identification error of EA does not affect the accuracy of the other identification parameters of H and EI because of the insensitivity itself to the frequencies in the proposed algorithm. To estimate the accurate axial rigidity from such bendable cable, the measurement of the axial frequencies may be necessary.

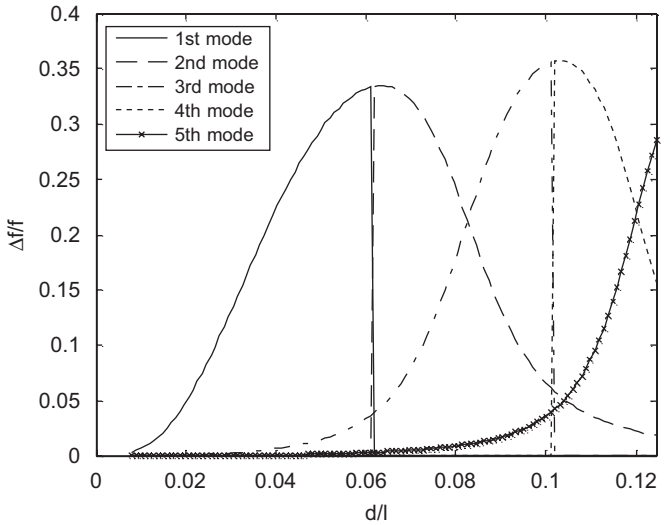

Fig. 11. The sensitivity of cable frequencies ($\Delta f/f$) to the axial rigidity EA with respect to the various sag-to-span ratios (d/l).

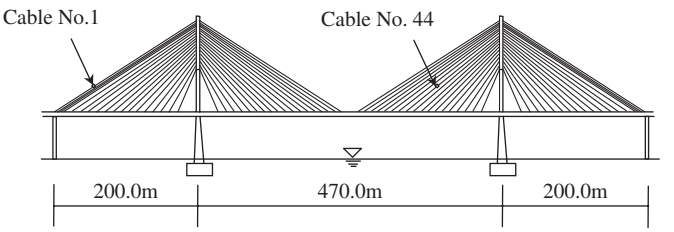

Fig. 12. Seohae cable-stayed bridge.

5. Field application

The Seohae cable-stayed bridge, built in 2000, is one part of the 7.31 km-long Seohae bridge across Asan bay on the expressway linking Incheon and Mokpo along West Coast in Korea. As shown in Fig. 12, the cable-stayed bridge is 990 m long and it has total 144 stay cables. Since the bridge is the doorway of Pyungtaek harbor, it has a clearance of 62 m high and 470 m wide for the navigational requirements. For the on-line heath monitoring of the cables, the 24 accelerometers are attached to the specific cables [14]. The total four sets of time history data collected from the No. 1 and No. 44 cables are considered here. The cable No. 1 is the longest cable and is weak from vibration. The horizontal length, the height, the self-weight, and the angle of cable inclination of the cable No. 1 are $l = 200.68$ m, $h = 110.03$ m, $w = 1226.25$ N/m and $\theta = 27.74^\circ$, respectively. It is reported that the time history data collected from the cable No. 44 has the worst quality. The horizontal length, the height, the self-weight, and the angle of cable inclination of the cable No. 44 are $l = 131.31$ m, $h = 90.57$ m, $w = 794.61$ N/m, and $\theta = 33.22^\circ$, respectively. The cross sections of the cable No. 1 and No. 44 consist of the 91 wires with $\varnothing = 0.0157$ m, the 61 wires with $\varnothing = 0.0157$ m, respectively. For the wind excitation (average velocity of 4.23 m/s), the acceleration time responses of cables are obtained by piezoelectric-type accelometers with the sampling rate of 0.01 s for 10 min. The typical power spectrum density (NFFT = 2048, Hanning window) of the cable No. 1 for the Inchon direction is shown in Fig. 13. The lower 30 and 20 modes of the cable No. 1 and No. 44, respectively, are extracted by the TDD (Time Domain Decompositon by Kim et al [15]) and the ERADC (Eigen-System Realization Algorithm with Data Correlation by Juang [16]) techniques. Normally speaking, those statistical modal parameter estimation

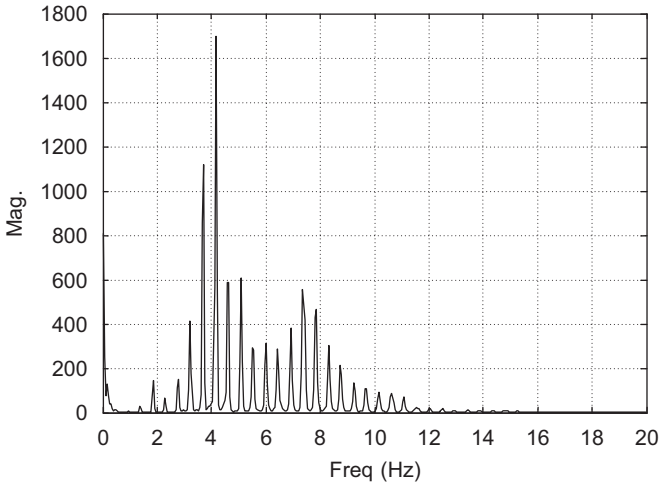

Fig. 13. Power spectrum density of Cable 1 in Seohae cable-stayed bridge.

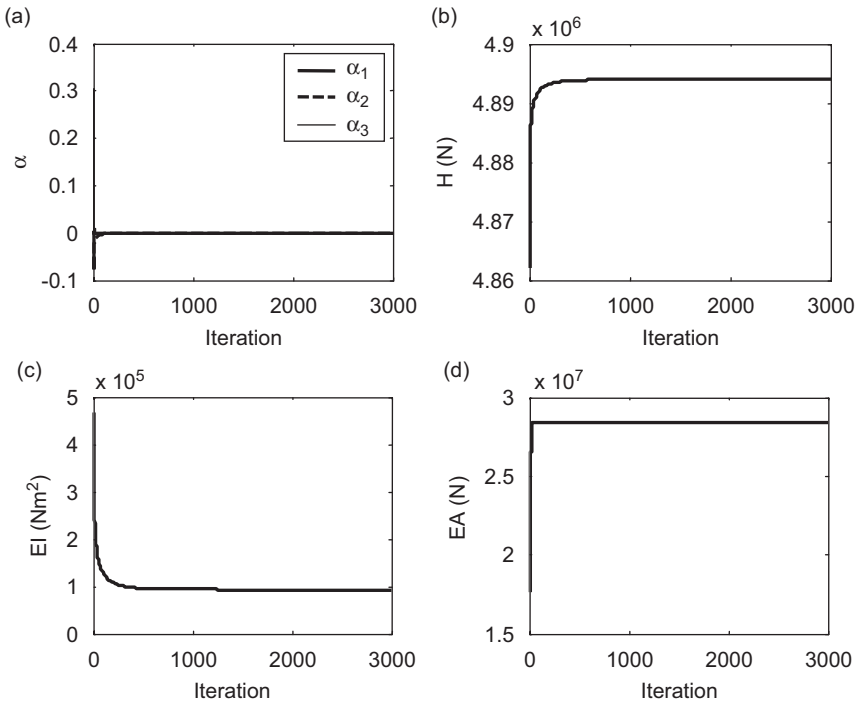

Fig. 14. Convergence of identification variables of Cable 1 in Seohae cable-stayed bridge: (a) fractional changes; (b) horizontal force component; (c) bending stiffness; and (d) axial stiffness.

methods significantly reduce uncertainty on the estimation of modal parameters, compared to the Pick-picking method. Here, the first lower modes of the cable No. 1 and No. 44 were not measured.

The proposed frequency-based system identification technique is applied to the extracted natural frequencies with a linear finite element cable model. The solution of sensitivity equation is obtained through the iteration method starting from arbitrary assumed initial values. As shown in Fig. 14, all the identification variables are converged through 3000 iterations. The estimation results using the proposed approach are listed in Table 7. For the case of the identified bending parameters, a large variation is observed, compared to that of

Table 7
Identified variables of Seohae Grand Bridge by the proposed method

	Cable no.			
	Cable 1		Cable 44	
Direction of lane	Inchon	Mokpo	Inchon	Mokpo
Horizontal force H (MN)	4.89	4.83	4.37	4.39
Flexural rigidity EI ($\times 10^4$ N m^2)	9.31	25.54	18.62	0.45
Axial rigidity EA (N $\times 10^7$)	2.84	1.73	1.10	1.11
Bending parameter ξ	1455.3	873.1	800.5	4313.9
Sag parameter λ^2	0.0147	0.0093	0.0021	0.0017

Table 8
Estimated tension forces of Seohae Grand Bridge (MN)

	Cable no.			
	Cable 1		Cable 44	
Direction of lane	Inchon	Mokpo	Inchon	Mokpo
Proposed approach	5.58	5.51	5.22	5.25
String theory (Eq. (1))	5.59	5.53	5.23	5.25
Russell et al. [4]	5.68	5.62	5.40	5.42
Linear regression (Eq. (2))	5.57	5.51	5.23	5.28
Zui et al. [5]	5.46	5.41	5.12	5.14
Static tensioning Jack	5.64	5.61	5.31	5.19

the identified horizontal force. The reason is due to the fact that the sensitivity of the tension force to the frequencies is relatively larger than that of the flexural rigidity. The partial evidence is that all the identified bending parameters are larger than 800. Furthermore, all the identified sag-extensibility parameters are nearly zero. Hence, the cable No. 1 and No. 44 could be classified as a cable system with small sag and low bending stiffness (Fig. 14).

For the extracted natural frequencies of Cable 1 and Cable 44, the aforementioned existing methods are applied. The estimated average tension forces are summarized in Table 8. The last row in Table 8 shows tension force measured by a tensioning hydraulic jack at August in 2000 [14]. Here, the difference of tension force between the deck side and the pylon side is about 2%. Unlike the results of the previous laboratory test, all the estimated tension forces show very good agreements. This is because the cable system considered here has very small sag and low bending stiffness due to the high level of tension force.

6. Summary and conclusions

The objective of this work is to introduce a new approach to estimate the cable tension forces from the measured frequencies. To achieve this objective, the following five basic steps were performed. First, the existing vibration-based tension estimation methods were classified as four categories, and their theoretical backgrounds were revisited. Second, the frequency-based system identification algorithm was presented in order to identify cable tension forces from measured frequencies. Third, the proposed approach was numerically verified using four case studies. The numerical study examined the effects of the sag-extensibility and bending stiffness on the performance of the proposed approach. Forth, the proposed approach was experimentally verified using a laboratory model. Finally, a feasibility study to data collected from Seohae cable-stayed bridge was presented.

Based on results and interpretations, the following five conclusions can be made. First, the cable tension forces estimated by the taut string theory and the modern cable theory are unreliable for the cables with high bending stiffness. However, the proposed method is capable of estimating the reliable tension forces for such bendable cables. Second, the reliable estimation of cable tension force by the linear regression approach requires the higher modes for a large sagged cable. This restriction could be an obstacle to estimate tension force if the higher modes of a cable could not be excited. However, the proposed method is able to reliably estimate the tension forces using only a few of lower modes. Third, unlike the methods using the practical formulas involving the sag-extensibility and bending stiffness, the proposed method does not require any priori knowledge about bending stiffness, axial rigidity, sag-to-span ratio, and unstrained length of cable. Fourth, the proposed approach could be applied to any cable system whose closed form solution is not available by virtue of utilizing the finite element analysis. Fifth, the bending stiffness of cables could be linearly proportional to the applied tension forces. This finding is not originally intended to be unveiled in this study. The detailed investigation of this phenomenon remains to be done.

Acknowledgment

The authors gratefully acknowledge the final support by Samsung Engineering & Construction. The authors also appreciate that Korean Highway Corporation have granted us permission to use the field data collected from Seohae cable-stayed bridge.

References

[1] H.M. Irvine, *Cable Structures*, The MIT Press, Cambridge, MA, 1981.
[2] M.S. Triantafyllou, The dynamics of taut inclined cables, *Quarterly Journal of Mechanics and Applied Mathematics* 37 (3) (1984) 421–440.
[3] M.S. Triantafyllou, L. Grinfogel, Natural frequencies and modes of inclined cables, *Journal of Structural Engineering, ASCE* 112 (1) (1986) 139–148.
[4] J.C. Russell, T.J. Lardner, Experimental determination of frequencies and tension for elastic cables, *Journal of Engineering Mechanics, ASCE* 124 (10) (1998) 1067–1072.
[5] H. Zui, T. Shinke, Y.H. Namita, Practical formulas for estimation of cable tension by vibration method, *Journal of Structural Engineering, ASCE* 122 (6) (1996) 651–656.
[6] W.H.P. Yen, A.B. Mehrabi, H. Tabatabai, Evaluation of stay cable tension using a non-destructive vibration technique, *Proceedings of the 15th Structures Congress*, Vol. 1, ASCE, New York, 1997, pp. 503–507.
[7] A.B. Mehrabi, H. Tabatabai, Unified finite difference formulation for free vibration of cables, *Journal of Structural Engineering, ASCE* 124 (11) (1998) 1313–1322.
[8] J.R. Casas, A Combined method for measuring cable forces: the cable-stayed Alamillo Bridge, Spain, *Structural Engineering International, IABSE* 4 (1994) 235–240.
[9] Y.Q. Ni, J.M. Ko, G. Zheng, Dynamic analysis of large-diameter sagged cables taking into account flexural rigidity, *Journal of Sound and Vibration* 257 (2) (2002) 301–319.
[10] T. Shimada, K. Kimoto, S. Narui, Study on estimating tension of tied hanger rope of suspension bridge by vibration method, *Proceedings of the JSCE* 404 (I–11) (1989) 455–458 (in Japanese).
[11] N. Stubbs, A general theory of non-destructive damage detection in structures, in: H.H.H. Leipholz (Ed.), *Proceedings of the Second International Symposium on Structural Control*, University of Waterloo, Ontario, Canada, Martinus Nijhoff Publishers, Dordrecht, Netherlands, 1985, pp. 694–713.
[12] B.H. Kim, N. Stubbs, T. Park, Flexural damage index equations of a plate, *Journal of Sound and Vibration* 283 (2005) 341–368.
[13] J.S. Bendat, A.G. Piersol, *Engineering Applications of Correlation and Spectral Analysis*, Wiley, New York, 1980.
[14] J.C. Park, C.M. Park, P.Y. Song, Evaluation of structural behaviors using full scale measurements on the Seo Hae Cable-Stayed Bridge, *Korean Society of Civil Engineers* 24 (2A) (2004) 249–257 (in Koreans).
[15] B.H. Kim, N. Stubbs, T. Park, A new method to extract modal parameters using output-only responses, *Journal of Sound and Vibration* 282 (2005) 215–230.
[16] J.-N. Juang, *Applied System Identification*, Prentice Hall, Englewood Cliffs, NJ, 1994.